IEEE Photonics Journal
An IEEE Photonics Society Publication

Open Access

A Comparative Analysis on Fully Integrated Spectral Broadening of Kerr Frequency Combs

Volume 9, Number 5, October 2017

Jing Wang
Yuhao Guo
Henan Liu
Guifang Li, ***Fellow, IEEE***
Lin Zhang, ***Member, IEEE***

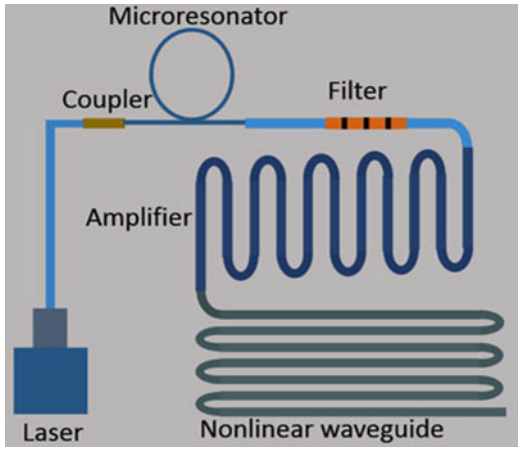

DOI: 10.1109/JPHOT.2017.2746675
1943-0655

IEEE photonics SOCIETY

IEEE

A Comparative Analysis on Fully Integrated Spectral Broadening of Kerr Frequency Combs

Jing Wang,[1,2] **Yuhao Guo,**[1,2] **Henan Liu,**[1,2]
Guifang Li,[1,2,3] ***Fellow, IEEE*, and Lin Zhang,**[1,2] ***Member, IEEE***

[1]Key Laboratory of Opto-electronic Information Technology of Ministry of Education, School of Precision Instrument and Opto-electronics Engineering, Tianjin University, Tianjin 300072, China
[2]Key Laboratory of Integrated Opto-electronic Technologies and Devices in Tianjin, School of Precision Instruments and Opto-electronics Engineering, Tianjin University, Tianjin, China
[3]CREOL, The College of Optics & Photonics, University of Central Florida, Orlando, FL 32816 USA

DOI:10.1109/JPHOT.2017.2746675

Manuscript received June 14, 2017; revised August 22, 2017; accepted August 23, 2017. Date of publication September 28, 2017; date of current version October 11, 2017. Corresponding author: Lin Zhang (e-mail: lin_zhang@tju.edu.cn).

Abstract: Microresonator-based frequency combs have potential to achieve on-chip frequency metrology. To obtain high-power comb lines at f and 2f for self-referenced stabilization, we evaluate the feasibility of building a fully integrated comb generator with spectral broadening. Comparing two types of nonlinear waveguides based on Si and chalcogenides, we find that the system feasibility relies on integrated waveguide amplifiers. If with a high-gain amplifier, a dispersion-engineered chalcogenide waveguide is preferred. Otherwise, an Si waveguide performs better. Considering the immaturity of both on-chip amplification technologies for ultrafast pulses and hybrid integration of multiple nonlinear materials, it could be concluded that in near future it is not practical to achieve fully on-chip f-2f self-referenced comb stabilization via subsequent spectral broadening of a Kerr frequency comb. Alternatively, direct generation of octave-spanning Kerr combs via dispersion engineering still remains attractive.

Index Terms: Integrated photonic system, Kerr effect.

1. Introduction

Stabilized broadband frequency combs enable many practical applications, e.g., optical signal processing, frequency metrology, and precision spectroscopy [1]. Octave-spanning combs with high comb-line powers at the spectrum edges for f-2f self-referencing [2] are critical for frequency metrology. Microcavity frequency combs, i.e., Kerr combs, exhibit great potential to make a frequency comb system compact and cost-effective [3]–[10]. Such a system includes many components: a pump laser, a nonlinear resonator, optical filters, amplifiers and detectors. It is thus desirable to have the entire system integrated on a single chip. On-chip frequency metrology in turn enables advanced functionalities such as portable timing/navigation units.

A mode-locked Kerr comb can be generated by tuning a pump laser into resonance and forming cavity solitons [11]. It is possible to obtain an octave-spanning mode-locked comb by

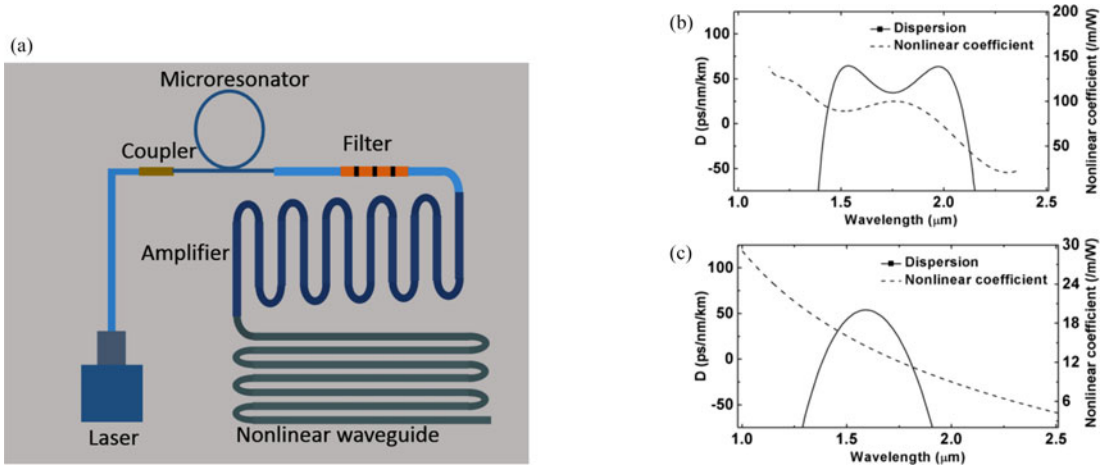

Fig. 1. (a) A fully integrated chip is studied for comb broadening, with an on-chip laser (with a SOA) of 130 mW, a Si_3N_4 cavity with a Q of 8×10^5, an optical amplifier, and a nonlinear waveguide. The parameters are set to be practical with the current integration technologies. Dispersion (solid) and nonlinearity (dashed) in the (b) Si and (c) GeSbS waveguide.

carefully tailoring the dispersion [12]–[14]. Alternatively, external spectral broadening of a Kerr comb was explored [11], [15], [16], achieving great broadening. The demonstrations adopted off-chip, fiber-based amplifiers and nonlinear media. It is of interest to evaluate the feasibility of realizing fully integrated comb spectral broadening for on-chip frequency metrology.

Here, we consider a Kerr comb with on-chip spectral broadening, in which the pump laser, optical amplifier and highly nonlinear waveguides are all feasible using the state-of-the-art technologies in integrated photonics. We study a Si_3N_4 cavity (often used for Kerr comb generation) as the nonlinear resonator and two types of nonlinear waveguides, with and without two-photon absorption (TPA) for spectral broadening. It can be seen that, even under the ideal condition for optical amplifiers (e.g., ignoring other practical issues such as gain fluctuation, coherence over the gain bandwidth, the insertion or connection losses, etc), both two types of waveguides show insufficient spectral power for f-2f stabilization limited by on-chip amplifier's performance. Operating conditions would be even more challenging when the above practical issues are taken into account. Alternatively, direct octave-spanning comb generation still remains attractive and feasible. More details are shown in the discussion session below.

2. System Configuration and Numerical Model

A typical configuration of nonlinear spectral broadening of frequency combs is shown in Fig. 1. An integrated CW pump laser using Si/III-V bonding technology [17], [18] is injected into a Si_3N_4 cavity to produce a narrowband mode-locked Kerr comb. The comb is amplified using an integrated optical amplifier and injected into a dispersion-tailored nonlinear waveguide to broaden its spectrum. The residual strong pump in the comb spectrum causes gain saturation. Thus, an on-chip filter [19] is inserted before the amplifier to remove the pump, and we choose to use the "through" port in the filter to block the pump and a small radius (e.g., 1.5 μm) for a filter to avoid repeated stop bands in the spectral range of interest. Or, one can add another bus waveguide to the Si_3N_4 cavity and use the "drop" port.

In our simulations, we specify these components to be compatible with the state of the art. The CW pump power (with a built-in semiconductor optical amplifier (SOA)) is set to be $\sim$130 mW [17], [18]. Pump linewidth can be narrowed down to $\sim$MHz by adding feedback control [20]. The Si_3N_4 cavity has an anomalous dispersion of -160 ps^2/km and a Q-factor of 8×10^5, the cavity loss is 0.2 dB/cm, and the coupling coefficient is 0.0037 [14]. Its free spectral range (FSR) is 200 GHz. One can use thermal tuning, with a high-speed detector, to measure the carrier envelope offset [21].

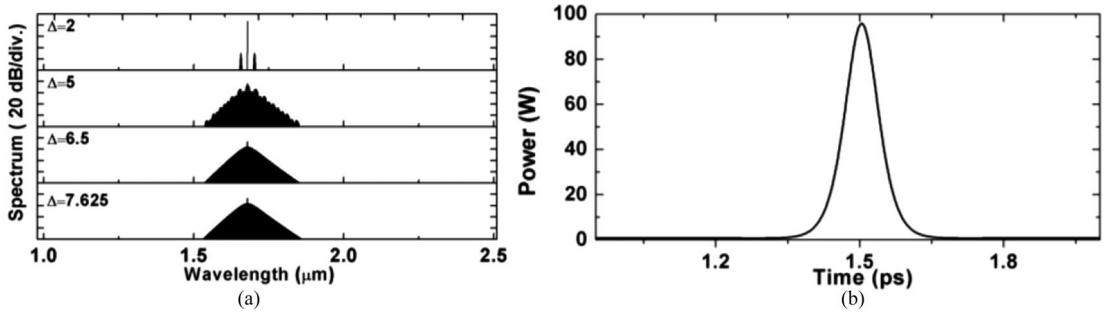

Fig. 2. (a) Spectrum evolution with the increasing red-detuning of the pump. (b) Stable soliton pulse waveform. Wavelength range is set to be the same as in Fig. 1(b) and (c).

There are a few options for integrated amplifiers including SOAs, Er-doped waveguide amplifiers, parametric amplifiers, and quantum dot amplifiers [22]–[27], most of which cannot provide sufficient gain and bandwidth for the generated mode-locked Kerr combs, associated with a femtosecond pulse train with a relatively high peak power. Electrically pumped quantum-dot amplifiers with a 40-dB gain might perform the best [25]–[27], although the published results are focused on the small signal input, with spectral coherence untested. Thus, in our simulation, we first consider the ideal amplification condition (with more detailed discussion given at the end of the paper), that is, the pulses are amplified with a spectrally uniform gain, assuming that the coherence of the pulses are not degraded, and also the insertion losses are temporally ignored.

Two types of highly nonlinear waveguides based on Si (with TPA) and chalcogenide glass (GeSbS, without TPA) are studied. We choose a Si slot waveguide [28] with width $W = 610$ nm, upper height $H_u = 133$ nm, lower height $H_l = 334$ nm, and slot height $H_s = 40$ nm. It has flattened dispersion shown in Fig. 1(b), facilitating spectrum broadening [28]. Using GeSbS, we design a strip waveguide (1200×500 nm^2) to obtain a proper dispersion in Fig. 1(c) for spectral broadening and dispersive wave generation at the spectral edges [2], f and 2f. Both waveguides are cm-long, with an optical loss of 2 and 0.5 dB/cm. To efficiently broaden the comb, we pump at 1.68 and 1.6 μm, respectively, the centers of the waveguides' anomalous dispersion regions, where the 2nd-order dispersion β_2 are -60 and -72 ps^2/km, and the nonlinear coefficients are 98 and 14 /W/m, which change with wavelength monotonically.

We use the Lugiato-Lefever equation to simulate the comb generation with a temporal step of 1 fs [11] and ignore higher-order dispersion, self-steepening and Raman effects, which are negligible if the Kerr comb is not broadband [28]. The nonlinear envelope equation is used to simulate the spectral broadening in the nonlinear waveguides as detailed in [28].

3. Results

With a pump of 130 mW, one can generate a mode-locked Kerr comb in the aforementioned Si_3N_4 cavity. The comb evolution is shown in Fig. 2(a), with an increasing pump detuning $\Delta = 2$, 5, 6.5, and 7.625 (Δ is defined as $2\delta_0/(\alpha + \kappa)$ [29]). The comb spectrum gradually becomes smooth, evolving from the modulational instability state to the cavity soliton state [28]. Fig. 2(b) shows the temporal profile of the stable cavity soliton at $\Delta = 7.625$, with a pulsewidth of 77 fs and a peak power of 96 W. Coupled out of the cavity, the pulse has a peak power of 290 mW, sitting on a 2.6 mW DC component, which is the residual pump after 20-dB attenuation by an optical bandstop filter. The optical amplifier is set to have a gain of 18.6 dB, resulting in the peak power P_0 of 20 W for the optical pulse launched into nonlinear waveguides, temporally ignoring other practical issues such as coherence over the gain bandwidth, the insertion/connection losses.

First, using the low-dispersion Si slot waveguide, we take TPA, free-carrier refraction and absorption into account, and the carrier lifetime is set to be 10 ps, which was realized by applying a reverse bias across the p-i-n waveguide structure [30]. In Fig. 3(a), the spectrum is broadened, and the

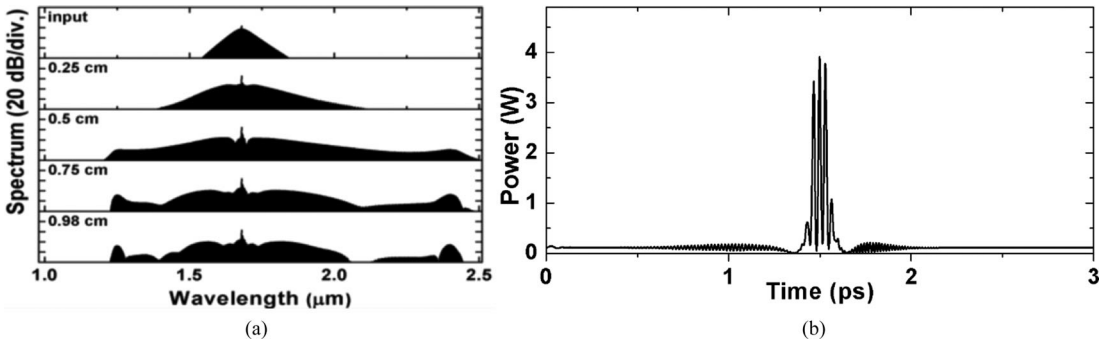

Fig. 3. (a) Spectrum of the pulse becomes broadened during the propagation and has two dispersive waves located at ~1.2 and 2.4 μm. (b) Pulse waveform generated at 0.98 cm.

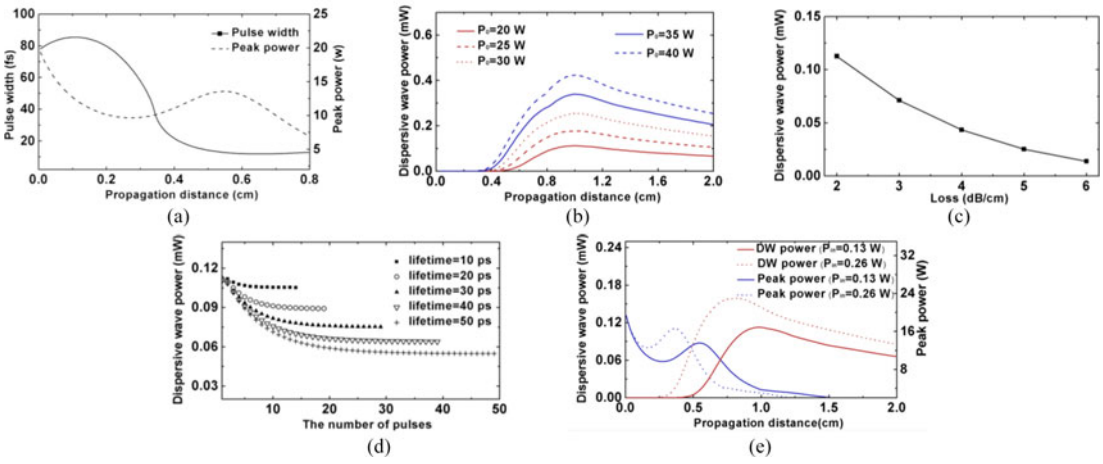

Fig. 4. (a) Pulse width (solid) and peak power (dashed) of the pulse as the function of the propagation distance. (b) Dispersive wave power vs. propagation distance, with varied peak powers of the pulse. The dispersive wave power reaches the highest value at 0.98 cm. (c) The dispersive wave power decreased from 0.113 to 0.014 mW as the scattering loss increases in the Si waveguide. (d) Dispersive wave power vs. the number of pulses for different lifetimes. (e) Dispersive wave power (blue lines) and peak power (red lines) changes with the propagation distance when the pump power is 0.13 W (solid lines) and 0.26 W (dashed lines).

comb line power located at 1.2 and 2.4 μm rises up, due to dispersive wave generation in the normal dispersion regions. The strong dispersive waves can be utilized for the f-2f self-referenced comb stabilization [2]. To do so, the dispersive wave at the low-frequency side needs to be frequency-doubled, requiring a higher power. Thus, the dispersive wave power around 2.4 μm is maximized at a propagation distance of 0.98 cm, as shown in Fig. 3(a). Fig. 3(b) shows the pulse waveform at 0.98 cm. As the dispersive waves slightly walk off from the pulse, there are some beating patterns at the rising and falling edges.

Fig. 4(a) shows the pulse width and peak power evolution along the waveguide up to a propagation distance of 0.8 cm, after which the pulse splits up. There is a slight pulse broadening first due to reduced peak power caused by TPA [28]. As the pulse propagates longer, it is greatly narrowed to a compression ratio of 4. The peak power decreases quickly with distance at first because of TPA and then rises up as a result of pulse compression. By varying the amplifier gain from 15 to 22 dB, one can increase the peak power from 10 to 40 W, while the low-frequency dispersive-wave power increases from 0.017 to 0.423 mW in the meantime, in Fig. 4(b). At a distance of $>$1 cm, the dispersive wave power decreases due to waveguide loss. We studied the effect of waveguide loss in Fig. 4(c). As the loss increases from 2 to 6 dB/cm, the dispersive wave is significantly suppressed from 0.113 to 0.014 mW.

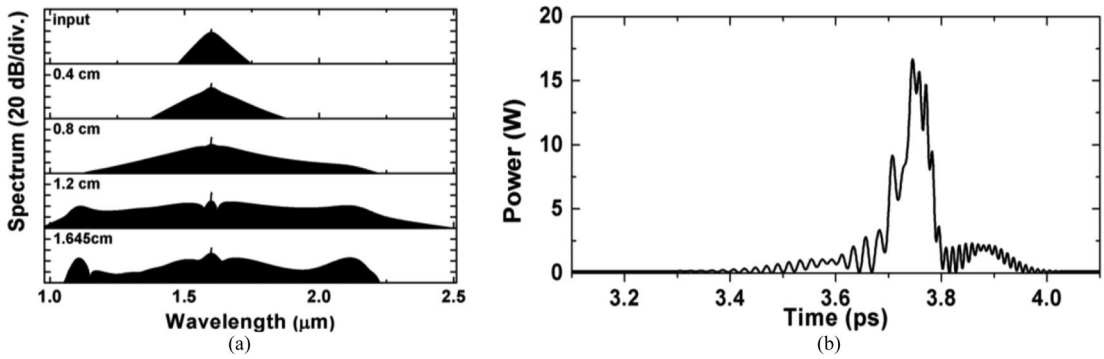

Fig. 5. (a) Spectrum of the pulse becomes broadened during the propagation and has two dispersive waves located at around 1.05 and 2.1 μm. (b) Pulse waveform generated at 1.645 cm.

We examine the impact of the carrier lifetime. Since mode-locked Kerr combs produce a pulse train with a relatively high repetition rate, free carriers generated due to TPA by preceding pulses reduce the peak power of subsequent pulses via free carrier absorption. One has to check a long-enough pulse train in the nonlinear pulse propagation. In Fig. 4(d), the dispersive wave power (free carrier concentration) decreases (increases) initially with the number of pulses before reaching a steady state. Then, the dispersive wave power is almost halved as the carrier lifetime increases from 10 to 50 ps, indicating the necessity of reducing the carrier lifetime [30]. To study the effect of the input pulse width on dispersive wave, we increased the pump power from 0.13 to 0.26 W, the cavity soliton pulsewidth is reduced to 58 fs. For a comparison, we amplify this input pulse to the same peak power at 20-W as before. In Fig. 4(e), the narrower pulse generates a higher dispersive wave power as a result of stronger self-phase modulation, thus making the spectrum wider. In contrast, with a pump power of 0.13 W, the soliton pulsewidth is 77-fs, corresponding to a larger pulse energy after amplification. However, TPA and free carrier absorption inhibit peak power build up during pulse compression, thus causing weaker dispersive waves, as shown in Fig. 4(e).

The dispersion-engineered GeSbS waveguide has no TPA but has a smaller nonlinear coefficient as compared to a Si waveguide. We amplify the soliton pulse from the cavity to the same peak power of 20 W. The comb spectral broadening is shown in Fig. 5(a). In this case, the dispersive waves are generated at 1.05 and 2.1 μm for f-2f self-referencing. We examine the dispersive wave at the low-frequency end, and its power reaches the highest at 1.645 cm. Accordingly, the temporal profile of the pulse is shown in Fig. 5(b), which is modulated due to the interference between the dispersive waves on both sides.

Fig. 6(a) shows pulse width and peak power along the GeSbS waveguide up to a propagation distance of 1.4 cm. It is clearly seen that the pulse is compressed greatly, up to a factor of 8. The peak power reaches 92 W during pulse compression, which is almost impossible with TPA such as in a Si waveguide. From Fig. 6(b), where the amplified peak power is varied from 10 to 40 W, one can observe that the dispersive wave power quickly rises up to a few mW, which is in a sharp contrast to that in the Si waveguide.

Fig. 6(c) shows the dispersive wave power versus the waveguide loss with a 20-W pulse peak power after amplification. Similar to the Si waveguide, the dispersive wave power decreases by more than one order of magnitude as the loss increasing from 0.2 to 3 dB/cm, showing the importance of the waveguide loss. Fig. 6(d) shows the comparison between the pump power of 0.13 W and 0.26 W, corresponding to a soliton pulsewidth of 77 and 55 fs, respectively. Note that the longer pulse generates a stronger dispersive wave during the pulse propagation, which is different from the case in Si waveguide. This is because the longer pulse can reach higher peak power after the pulse compression, in the absence of TPA.

Finally, in Fig. 7, we compare the powers of low-frequency dispersive waves in both the Si and GeSbS waveguides as functions of the pulse peak power, P_0, which is determined by the amplifier gain. When the gain is $\sim$14 dB, i.e., a pulse peak power of 7.5 W, the Si waveguide generates higher

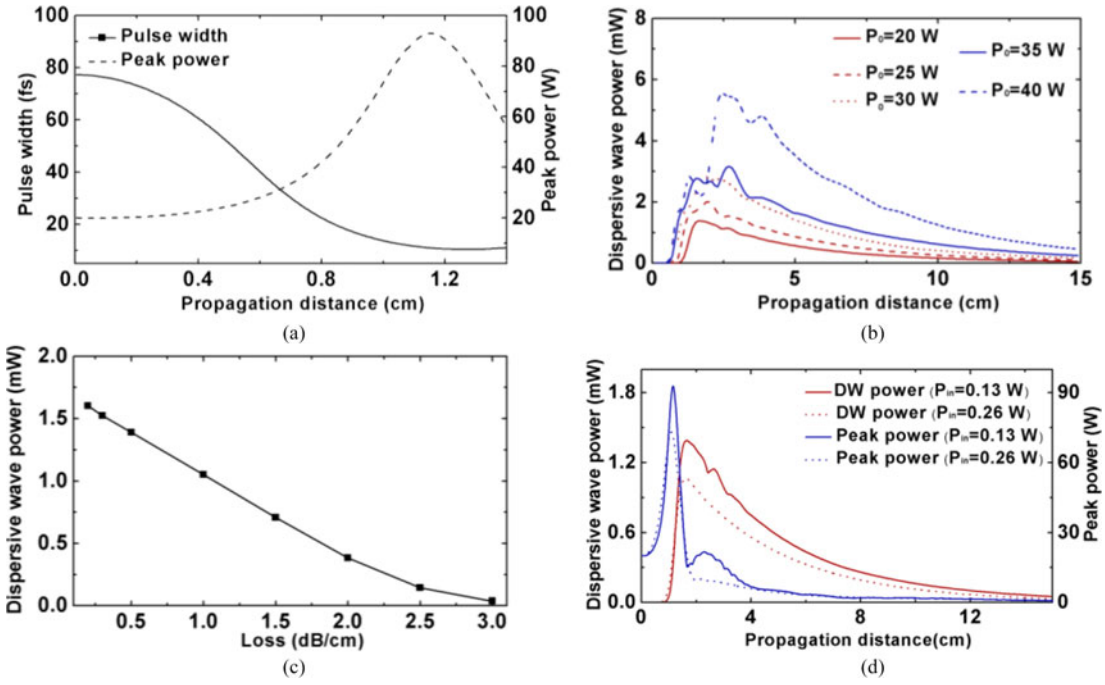

Fig. 6. (a). Pulse width (solid) and peak power (dashed) of the pulse as the function of the propagation distance. (b) Dispersive wave power vs. propagation distance, with varied peak powers of the pulse. (c) Calculated maximum dispersive wave power generated during the propagation as a function of the scattering loss in the GeSbS waveguide. (d) Dispersive wave power (blue lines) and peak power (red lines) changes with the propagation distance when the pump power is 0.13 W (solid lines) and 0.26 W (dash lines).

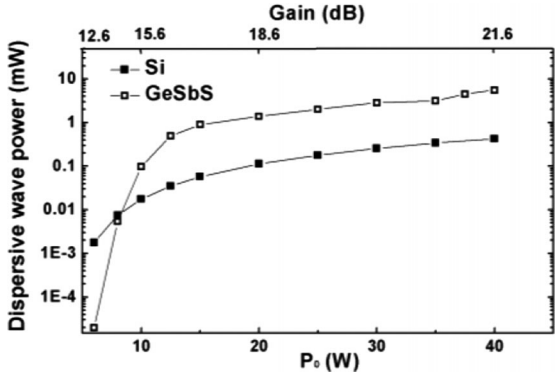

Fig. 7. The dispersive wave power changes with input peak power (amplification gain) in silicon (solid square) and GeSbS (empty square), respectively.

dispersive wave power due to the almost negligible TPA and free carrier absorption. However, the limited peak power restricts the dispersive wave generation of both waveguides with a maximum power of only 7.5 μW, which is far away from the sufficient power for frequency doubling for f-2f stabilization. When the amplifier gain reaches 18 dB or higher, the GeSbS waveguide shows stronger dispersive wave (even mW-level), which is desirable for frequency doubling and would make on-chip frequency metrology system more possible. However, this relies on the large amplifier gain on femtosecond pulses, which can be very challenging with the state-of-art technology.

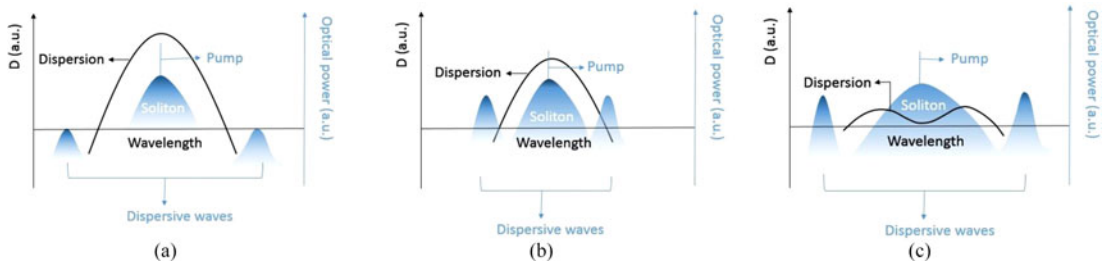

Fig. 8. Three types of dispersion profiles and the associated generated combs. Compared with (a), (b), the precisely designed dispersion profile in (c) is quite low and widely flattened and the corresponding generated comb is wide and powerful enough for f-2f self-reference.

4. Discussion

It is shown from above that even under the ideal condition set for the amplifiers in our simulation, both silicon and chalcogenide waveguides produce dispersive wave power at μW-level, when the amplifier gain is less than 14 dB, which is insufficient for on-chip frequency doubling for f-2f stabilization. A gain higher than 18 dB from the amplifier would make GeSbS waveguide more favorable, generating even mW-level dispersive wave. Nevertheless, such a large gain on femtosecond pulses can hardly be achieved with the state-of-art technology, considering a relatively high peak power of the pulses. Moreover, in a real amplifier, the gain spectrum is typically not uniform over the whole comb bandwidth (nearly 100 nm). The coherence over the gain bandwidth could also be problematic. Both issues are critical in determining the waveform distortion and frequency chirp of the femtosecond pulses before they are launched into nonlinear waveguides. In this sense, a high-performance integrated amplifier is the key to on-chip spectral broadening of Kerr combs for frequency metrology. Due to device fabrication and material choice, one should also include the insertion/connection losses between various devices, which add more difficulties to the system's realization. Special attention has to be paid to material compatibility and processing step modification. If chalcogenide devices are chosen, high-temperature processing would be avoided, since the chalcogenides have a low melting temperature.

Alternatively, the direct frequency comb generation still remains attractive and feasible. The key to broadband frequency comb generation is dispersion engineering. The dispersion of the waveguide usually have two zero dispersion points and is used in two ways as shown in Fig. 8(a) and (b). In Fig. 8(a), the generated soliton experiences large and broadband anomalous dispersion. Accordingly, the generated dispersive waves can be far apart, separated by one octave. However, due to a narrow bandwidth of the soliton, the dispersive waves have fairly low power, which is not sufficient for frequency doubling. Instead in Fig. 8(b), the dispersion can be relatively low and accordingly the anomalous bandwidth is also small. As a consequence, two dispersive waves become stronger but are close to each other, making it impossible for f-2f comb stabilization. In this sense, desired dispersion profile would have two zero-dispersion points widely separated but low dispersion in the middle, i.e., a saddle-shaped curve [12], in order to obtain high-power dispersive waves located at f and 2f frequencies. This can be explained as follows. In [29], the 3 dB comb bandwidth is expressed as:

$$\Delta f_{theo} = \frac{0.315}{1.763}\sqrt{\frac{2\gamma P_{in}\mathcal{F}}{\pi\,|\beta_2|}}$$

which indicates that a broad and low dispersion would facilitate octave-spanning comb generation [12]. As a result, the f and 2f frequency components in a soliton spectrum are strong, favorably seeding dispersive wave generation. The ultimately designed dispersion profile is illustrated in Fig. 8(c), which is fairly low and widely flattened. Accordingly, the generated comb with the proper dispersive waves can be octave-spanning and well-flattened shown in Fig. 8(c). In [12], it's shown that even two-cycle pulses can be generated, when the dispersion is properly engineered, which

would be desirable for frequency metrology application. Now there are several groups ([12], [31], [32]) working on this proposal, which can potentially produce relatively high dispersive wave power for self-reference and also are based on a simpler system.

5. Summary

In this work, we study on-chip spectral broadening of Kerr frequency combs featured by dispersive wave generation. Given all the technical challenges considered, we believe that subsequent spectral broadening of Kerr combs for on-chip frequency metrology is currently unfeasible, and direct generation of octave-spanning Kerr combs, as a promising alternative, still remains strongly attractive.

Acknowledgment

This work is supported in part by the National Basic Research Program of China (973) Project #2014CB340104/3, NSFC Projects 61775164, 61335005, 61377076, 61575142 and 61431009.

References

[1] J. Ye and S. T. Steven, *Femtosecond Optical Frequency Comb Technology: Principle, Operation, and Applications*. New York, NY, USA: Springer, 2005.
[2] T. Udem, R. Holzwarth, and T. W. Hansch, "Optical frequency metrology," *Nature*, vol. 416, no. 6877, pp. 233–237, Mar. 2002.
[3] T. J. Kippenberg, R. Holzwarth, and S. A. Diddams, "Microresonator-based optical frequency combs," *Science*, vol. 332, pp. 555–559, Apr. 2011.
[4] J. S. Levy, A. Gondarenko, M. A. Foster, A. C. Turner-Foster, A. L. Gaeta, and M. Lipson, "CMOS-compatible multiple-wavelength oscillator for on-chip optical interconnects," *Nature Photon.*, vol. 4, no. 1, pp. 37–40, Dec. 2010.
[5] F. Ferdous *et al.*, "Spectral line-by-line pulse shaping of on-chip microresonator frequency combs," *Nature Photon.*, vol. 5, pp. 770–776, Oct. 2011.
[6] S.-W. Huang *et al.*, "Mode-locked ultrashort pulse generation from on-chip normal dispersion microresonators," *Phys. Rev. Lett.*, vol. 114, no. 5, pp. 053901-1–053901-5, Feb. 2015.
[7] P.-H. Wang *et al.*, "Observation of correlation between route to formation, coherence, noise, and communication performance of Kerr combs," *Opt. Express*, vol. 20, no. 28, pp. 29284–29295, Dec. 2012.
[8] T. Hansson, D. Modotto, and S. Wabnitz, "Mid-infrared soliton and Raman frequency comb generation in silicon microrings," *Opt. Lett.*, vol. 39, no. 23, pp. 6747–6750, Dec. 2014.
[9] S. B. Papp and S. A. Diddams, "Spectral and temporal characterization of a fused-quartz-microresonator optical frequency comb," *Phys. Rev. A*, vol. 84, no. 5, pp. 053833-1–053833-7, Nov. 2011.
[10] Y. K. Chembo, D. V. Strekalov, and N. Yu, "Spectrum and dynamics of optical frequency combs generated with monolithic whispering gallery mode resonators," *Phys. Rev. Lett.*, vol. 104, no. 10, pp. 103902-1–103902-4, Mar. 2010.
[11] T. Herr *et al.*, "Temporal solitons in optical microresonators," *Nature Photon.*, vol. 8, pp. 145–152, Feb. 2014.
[12] L. Zhang *et al.*, "Generation of two-cycle pulses and octave-spanning frequency combs in a dispersion-flattened micro-resonator," *Opt. Lett.*, vol. 38, no. 23, pp. 5122–5125, Dec. 2013.
[13] I. S. Grudinin and N. Yu, "Towards efficient octave-spanning comb with micro-structured crystalline resonator," *Proc. SPIE*, vol. 93430, 2015.
[14] Y. Okawachi, K. Saha, J. S. Levy, Y. H. Wen, M. Lipson, and A. L. Gaeta, "Octave-spanning frequency comb generation in a silicon nitride chip," *Opt. Lett.*, vol. 36, no. 17, pp. 3398–3400, Sep. 2011.
[15] Y. Liu *et al.*, "Spectral broadening of Kerr Frequency combs generated from a normal dispersion silicon nitride microresonator," in *Proc. Lasers Electro-Optics: Science and Innovations*, 2015, Paper no. STh4N-3.
[16] S. B. Papp *et al.*, "Microresonator frequency comb optical clock," *Optica*, vol. 1, no. 1, pp. 10–14, Jul. 2014.
[17] M. N. Sysak *et al.*, "Hybrid silicon laser technology: a thermal perspective," *IEEE J. Sel. Topics Quantum Electron.*, vol. 17, no. 6, pp. 1490–1498, Apr. 2011.
[18] K. Morito and S. Tanaka, "Record high saturation power (+22 dBm) and low noise figure (5.7 dB) polarization-insensitive SOA module," *IEEE Photon. Technol. Lett.*, vol. 17, no. 17, pp. 1298–1300, Jun. 2005.
[19] Q. Xu, D. Fattal, and R. G. Beausoleil, "Silicon microring resonators with 1.5-μm radius," *Opt. Express*, vol. 16, no. 6, pp. 4309–4315, Mar. 2008.
[20] M. Bagheri, F. Aflatouni, A. Imani, A. Goel, and H. Hashemi, "Semiconductor laser phase-noise cancellation using and electrical feed-forward scheme," *Opt. Lett.*, vol. 34, no. 19, pp. 2979–2981, Oct. 2009.
[21] X. Xue *et al.*, "Thermal tuning of Kerr frequency combs in silicon nitride microring resonators," *Opt. Express*, vol. 24, no. 1, pp. 687–698, Jan. 2016.
[22] K. H. Lin and J. H. Lin, "Amplification of supercontinuum by semiconductor and Er-doped fiber optical amplifiers," *Laser Phys. Lett.*, vol. 5, no. 6, pp. 449–453, Mar. 2008.
[23] K. Vu, S. Farahani, and S. Madden, "980 nm pumped erbium doped tellurium oxide planar rib waveguide laser and amplifier with gain in S, C and L band," *Opt. Express*, vol. 23, no. 2, pp. 747–755, Jan. 2015.

[24] B. Kuyken *et al.*, "On-chip parametric amplification with 26.5 dB gain at telecommunication wavelengths using CMOS-compatible hydrogenated amorphous silicon waveguides," *Opt. Lett.*, vol. 36, no. 4, pp. 552–554, Feb. 2011.
[25] G. Contestabile, Y. Yoshida, A. Maruta, and K. Kitayama, "Ultra-broad band, low power, highly efficient coherent wavelength conversion in quantum dot SOA," *Opt. Express*, vol. 20, no. 25, pp. 27902–27907, Nov. 2012.
[26] S. Lang, G. Contestabile, Y. Yoshida, A. Maruta, and K. Kitayama, "Phase-transparent amplification of 16 QAM Signals in a QD-SOA," *IEEE Photon. Technol. Lett.,* vol. 25, no. 24, pp. 2486–2489, Dec. 2013.
[27] G. Contestabile, A. Maruta, and K. Kitayama, "Four Wave Mixing in Quantum Dot Semiconductor Optical Amplifiers," *IEEE J. Sel. Topics Quantum Electron.*, vol. 50, no. 5, pp. 379–389, May 2014.
[28] L. Zhang *et al.*, "On-chip octave-spanning supercontinuum in nanostructured silicon waveguides using ultralow pulse energy," *IEEE J. Sel. Topics Quantum Electron.*, vol. 18, no. 6, pp. 1799–1806, Nov. 2012.
[29] S. Coen and M. Erkintalo, "Universal scaling laws of Kerr frequency combs," *Opt. Lett.*, vol. 38, no. 11, pp. 1790–1792, Jun. 2013.
[30] A. C. Turner-Foster *et al.*, "Ultrashort free-carrier lifetime in low-loss silicon nanowaveguides," *Opt. Express*, vol. 18, no. 4, pp. 3582–3591, Feb. 2010.
[31] V. Brash *et al.*, "Photonic chip-based optical frequency comb using soliton Cherenkov radiation," *Science*, vol. 351, no. 6271, pp. 357–360, 2016.
[32] Q. Li *et al.*, "Octave-spanning microcavity Kerr frequency combs with harmonic dispersive-wave emission on a silicon chip," in *Proc. Frontiers Opt.*, 2015, Paper no. FW6C.5.